Original Article | **Open Access**

Vessel Plus

Lin *et al. Vessel Plus.* 2026;10:48 **DOI:**10.20517/2574-1209.2025.162

Plasma proteomic profiling reveals potential biomarkers for sinus node dysfunction in persistent atrial fibrillation

Tianyi Lin#, Taojie Zhou#, Yongying Lan#, Qingzhi Luo, Yue Wei, Changjian Lin, Yangyang Bao, Qi Jin, Ning Zhang, Liqun Wu, Yun Xie

Keywords:
Proteomics, sinus node dysfunction, persistent atrial fibrillation, weighted gene co-expression network analysis, acid phosphatase 5

Citation: Lin T, Zhou T, Lan Y, Luo Q, Wei Y, Lin C, Bao Y, Jin Q, Zhang N, Wu L, Xie Y. Plasma proteomic profiling reveals potential biomarkers for sinus node dysfunction in persistent atrial fibrillation. *Vessel Plus.* 2026;10:48. https://dx.doi.org/10.20517/2574-1209.2025.162

Received: 21 Dec 2025 **First Decision:** 29 May 2026 **Revised:** 12 Jun 2026 **Accepted:** 7 Aug 2026 **Published:** 31 Aug 2026

Academic Editor: Yajun Duan
Copy Editor: Fangling Lan
Production Editor: Fangling Lan

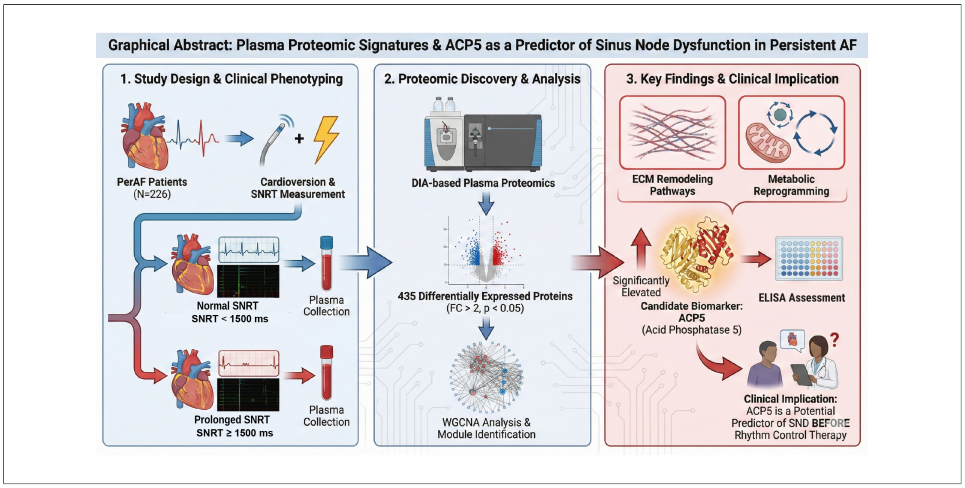

Abstract

Aims: In patients with persistent atrial fibrillation (PerAF), detecting sinus node dysfunction (SND) before rhythm control therapy is challenging, which may increase the risk of post-cardioversion bradyarrhythmia and complicate clinical management. This study aimed to identify plasma proteomic signatures associated with prolonged sinus node recovery time (SNRT) and to explore potential predictors of SND in PerAF patients.

Methods: A total of 226 consecutive patients with PerAF undergoing catheter ablation were screened, and 177 eligible patients were included. SNRT was measured after cardioversion, with 1,500 ms used as the cutoff to define prolonged SNRT. Propensity score matching was applied to select matched controls. Plasma samples were analyzed using proteomic techniques to compare protein expression profiles between the prolonged-SNRT and normal-SNRT groups. A weighted gene co-expression network analysis (WGCNA) was conducted to determine the most significant module and hub proteins associated with SNRT. An enzyme-linked immunosorbent assay was used for further assessment of candidate biomarkers.

Department of Cardiovascular Medicine, Ruijin Hospital, Shanghai Jiao Tong University School of Medicine, Shanghai 200025, China.
#Authors contributed equally.

Correspondence to: Dr. Ning Zhang, Dr. Liqun Wu, Dr. Yun Xie, Department of Cardiovascular Medicine, Ruijin Hospital, No. 197, Ruijin Er Road, Shanghai 200025, China. E-mail: zn11476@rjh.com.cn; wlq10583@rjh.com.cn; xy11992@rjh.com.cn

Results: Proteomic analysis identified 435 differentially expressed proteins, including 138 upregulated and 297 downregulated proteins in the prolonged-SNRT group. Integrated data-independent acquisition-based proteomics and WGCNA revealed a distinct plasma proteomic signature associated with prolonged SNRT in patients with PerAF, characterized by enrichment of extracellular matrix remodeling and metabolic reprogramming pathways. Acid phosphatase 5 (ACP5) was selected as a candidate biomarker, which was significantly elevated in patients complicated by SND in the validation set.

Conclusions: This study revealed distinct plasma proteomic features in PerAF patients with prolonged SNRT. ACP5 may serve as a potential biomarker to assess sinoatrial node function in PerAF patients prior to rhythm control therapy.

INTRODUCTION

Sinus node dysfunction (SND) and atrial fibrillation (AF) often occur together, forming a tachycardia-bradycardia syndrome, symptomatic bradycardia, or prolonged pauses after termination of atrial tachyarrhythmias, sometimes necessitating pacemaker implantation[1-3]. Epidemiological studies show that up to 50% of patients with SND concurrently present with AF[4], while AF can exacerbate SND through progressive atrial electrical and structural remodeling[5]. These conditions share a reciprocal, self-sustaining relationship: AF promotes atrial remodeling and fibrosis that impairs sinus node function, while intrinsic SND creates an electrophysiological environment conducive to AF[6]. Histopathological studies have demonstrated interstitial fibrosis and inflammatory cell infiltration in the sinus node region of patients with AF and SND[5]. However, the molecular alterations associated with impaired sinus node function in patients with AF remain incompletely understood.

In clinical practice, rhythm control therapy has become an increasingly important component of the treatment of patients with AF. However, evaluation of sinus node function is clinically challenging in patients with persistent atrial fibrillation (PerAF). When AF terminates in these patients, severe sinus bradycardia or even sinus arrest may occur, especially in those with prolonged sinus node recovery time (SNRT) after restoration of sinus rhythm, posing risks to patients and complicating subsequent clinical management. Given the difficulty in obtaining clinical specimens from the sinoatrial node region, identifying circulating biomarkers may offer a practical approach to investigating the molecular alterations associated with sinus node functional impairment. However, no reliable molecular markers have been established. Previous studies have focused on a limited number of candidate biomarkers or genetic variants[6-8], leaving the broader circulating proteomic landscape associated with SND in the PerAF population largely unexplored.

High-throughput proteomics has become a powerful tool for characterizing disease-related molecular signatures by simultaneously measuring thousands of plasma proteins in cardiovascular research[9,10]. However, studies investigating circulating proteomic alterations related to SND in AF remain limited. In addition to traditional single-protein comparisons, recently developed weighted gene co-expression network analysis (WGCNA) enables the identification of modules of co-regulated proteins that are functionally connected and linked to specific phenotypes[11]. Combining proteomic profiling with WGCNA provides a systems-level approach to reveal molecular changes associated with impaired sinus node function.

In this study, we aimed to define the plasma proteomic profile associated with prolonged SNRT in patients with PerAF using a propensity score-matched clinical cohort. By integrating differential protein expression analysis with WGCNA, we sought to identify functionally related protein modules and candidate circulating

biomarkers associated with prolonged SNRT and sinoatrial node function.

METHODS

Study design and population

A total of 226 consecutive patients were initially screened in this single-center, observational study. All patients with symptomatic, drug-refractory PerAF underwent first-time catheter ablation between July and December 2024 at the Department of Cardiovascular Medicine, Ruijin Hospital, Shanghai Jiao Tong University School of Medicine. Additional inclusion criteria included: age ≥ 18 years, left atrial diameter between 40 and 50 mm, and no documented history of other arrhythmias, including supraventricular tachycardia and atrial flutter. Exclusion criteria included: (1) structural heart disease other than hypertensive or ischemic heart disease; (2) prior pacemaker implantation or known congenital conduction disorder; (3) severe hepatic or renal dysfunction; and (4) active infection or malignancy at enrollment. The patient screening, enrollment, and grouping process is summarized in Figure 1. Written informed consent was obtained from all participants prior to enrollment. The study protocol conformed to the Declaration of Helsinki and was approved by the Institutional Ethics Committee of Ruijin Hospital, Shanghai Jiao Tong University School of Medicine (Approval No. 2021-139).

Ablation procedure and SNRT measurement

Following discontinuation of antiarrhythmic drugs for at least five half-lives, patients underwent catheter ablation under conscious sedation. Pre-procedural evaluations, including transthoracic and transesophageal echocardiography, were routinely performed. A decapolar catheter and a bipolar catheter (St Jude Medical, Inc, St. Paul, MN) were placed within the coronary sinus and at the right ventricular apex, respectively. The surface electrocardiogram (ECG) and bipolar endocardial electrograms were continuously monitored and recorded using a computer-based digital amplifier and recording system (Bard Electrophysiology). Intravenous heparin was administered to maintain an activated clotting time of > 250 s during the procedure.

Radiofrequency or cryoballoon ablation was performed according to the operator's preference. As a standard procedure, pulmonary vein electrical isolation (PVI) was conducted in all patients as the initial ablation strategy. After completion of PVI, a single synchronized biphasic shock (typically 100-200 J) was performed to restore sinus rhythm in all patients. SNRT was defined as the interval from the cardioversion artifact (time 0) to the onset of the first spontaneous sinus P wave observed on the surface ECG and confirmed by intracardiac electrograms. Prolonged SNRT was defined as ≥ 1,500 ms[12,13]. Patients were classified into the normal-SNRT group and the prolonged-SNRT group according to SNRT duration. Additional ablation procedures were performed subsequently based on the patient's clinical condition.

Propensity score matching (PSM)

To enhance comparability between patients with prolonged SNRT and those with normal SNRT, PSM was performed. The probability of prolonged SNRT was estimated using a multivariable logistic regression model that incorporated age, sex, body mass index, hypertension, diabetes mellitus, coronary artery disease, previous stroke or transient ischemic attack, left atrial diameter, and left ventricular ejection fraction. Patients were paired in a 1:1 ratio using nearest-neighbor matching without replacement, with a caliper set at 0.2 standard deviations (SDs) of the logit of the propensity score. Post-matching balance was assessed using absolute standardized mean differences, and values < 0.10 were considered indicative of satisfactory balance.

Plasma sample collection and proteomic analysis

For the proteomic discovery analysis, 10 participants were randomly chosen from the propensity score-matched population, including five with prolonged SNRT and five with normal SNRT. Fasting venous blood was obtained before ablation using ethylenediaminetetraacetic acid-containing tubes. Following

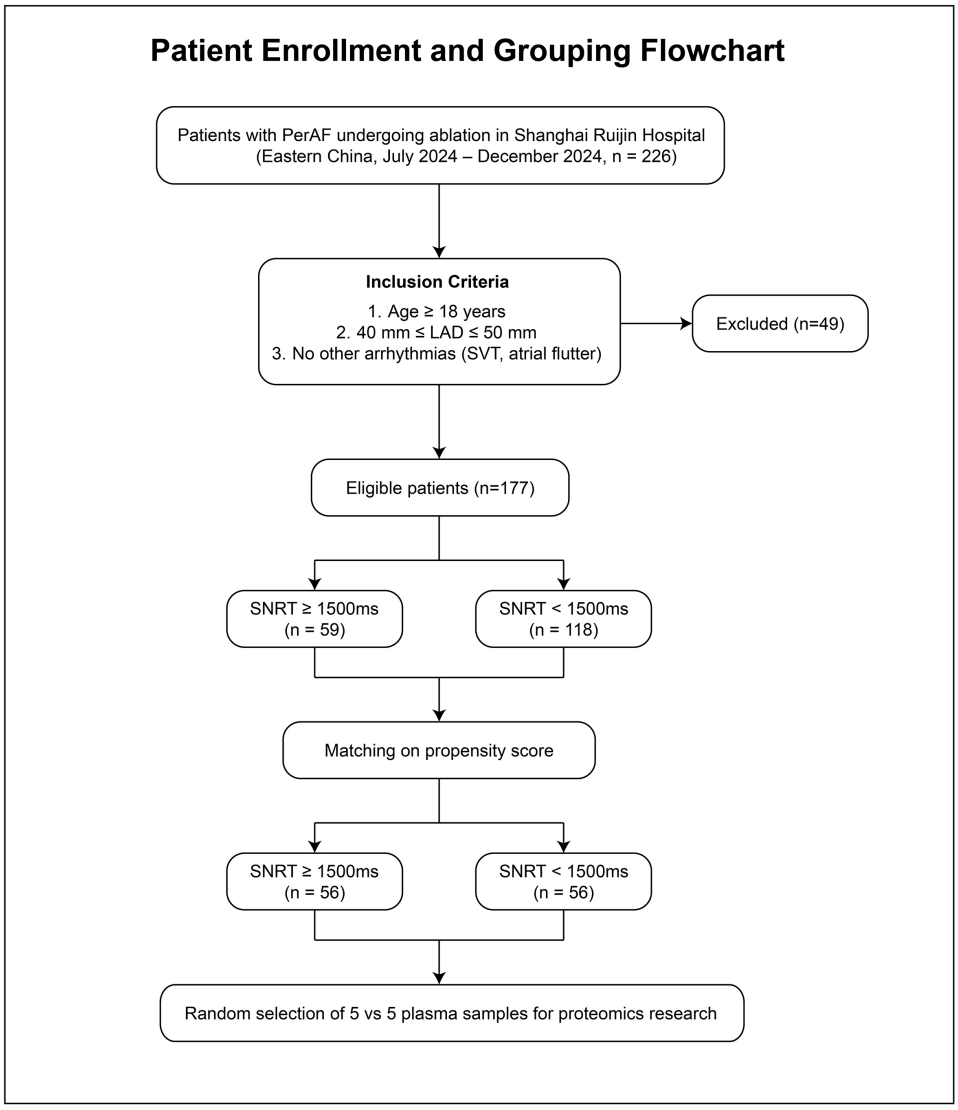

Figure 1. Flowchart of patient selection and inclusion in the proteomic analysis. Flow diagram illustrating the selection of patients with persistent atrial fibrillation (PerAF) who underwent ablation at Ruijin Hospital (Shanghai, China) between July and December 2024. Patients with a left atrial diameter (LAD) ranging from 40 to 50 mm were included whereas those with other arrhythmias (e.g., supraventricular tachycardia or atrial flutter) were excluded. Eligible patients (n = 177) were stratified according to SNRT. After propensity score matching, 56 patients were included in each group. Peripheral blood samples from five matched pairs were randomly selected for proteomic analysis. PerAF: Persistent atrial fibrillation; LAD: left atrial diameter; SNRT: sinus node recovery time.

centrifugation at 3,000 rpm for 10 min at 4 °C, plasma was aliquoted and kept at -80 °C until further analysis.

Briefly, low-abundance plasma proteins were enriched using a proprietary magnetic nanoparticle-based enrichment platform (OE Biotech Co., Ltd., Shanghai, China). After incubation at 37 °C for 1 h, washing steps were performed to remove non-specifically bound plasma proteins. The captured proteins were subsequently denatured, reduced, alkylated, and enzymatically digested at 37 °C for 2 h. Peptides were then purified using C18 spin columns, vacuum-concentrated, and quantified. Following addition of iRT standards at 1:20 (v/v), peptides were separated on an EASY-nLC 1200 system (Thermo Fisher Scientific, Waltham, MA, USA) using a 60-min gradient and analyzed by data-independent acquisition (DIA) on a timsTOF Pro mass spectrometer (Bruker Daltonics, Bremen, Germany). The main acquisition settings were 1.4 kV capillary voltage, 180 °C drying-gas temperature, m/z 100-1,700, and an ion-mobility range of 0.7-1.3 V·s/cm^2. Raw data were processed in Spectronaut 18.4 (Biognosys, Schlieren, Switzerland). Differentially

expressed proteins (DEPs) were defined as those with a fold change > 2.0 or < 0.5 and a nominal *P* value < 0.05. *P* values were not adjusted for multiple comparisons.

Functional enrichment and protein interaction analyses

Functional enrichment analyses of DEPs were performed using clusterProfiler (version 4.8.3) with annotations from the Gene ontology (GO) and Kyoto Encyclopedia of Genes and Genomes (KEGG) databases. GO terms were categorized into biological process (BP), cellular component (CC), and molecular function (MF). Adjusted *P*-values were computed using Benjamini-Hochberg correction for multiple testing. Protein-protein interaction networks were constructed using the STRING database (version 12.0) with an interaction confidence score threshold of 0.7. The resulting networks were visualized in Cytoscape (version 3.10). Hub proteins were identified according to degree centrality, defined as the top 10% of nodes ranked by interaction count.

WGCNA analysis

To identify coordinated protein modules correlated with prolonged SNRT, WGCNA was applied to the proteomic abundance data. Pearson correlations were calculated among the retained proteins and subsequently converted into weighted connection strengths using a soft-thresholding parameter β. The value of β was chosen to obtain an approximate scale-free network topology, with a fit index of 0.90. The adjacency matrix was converted to a topological overlap matrix, and proteins were hierarchically clustered according to topological overlap dissimilarity using the average-linkage method. Protein modules were delineated from the resulting dendrogram with the dynamic tree-cut procedure, using a minimum module size of 40, and were denoted by different colors. The first principal component of each module, referred to as the module eigengene, was calculated and correlated with the binary SNRT phenotype, coded as 1 for prolonged SNRT and 0 for normal SNRT. Module-trait correlations were visualized in a heatmap. Gene significance (GS, representing protein significance in this context) and module membership (MM) were computed for each protein. The relationship between GS and MM was plotted to identify hub proteins strongly associated with both network topology and the prolonged-SNRT phenotype. GO and KEGG enrichment analyses were repeated for key modules to determine biological themes associated with prolonged SNRT and impaired sinus node recovery function.

Validation by enzyme-linked immunosorbent assay (ELISA)

Based on its relevance to cardiac remodeling and its position within the WGCNA-identified module, Acid phosphatase 5 (ACP5) was selected for validation in the full matched cohort (n = 112). Plasma concentrations were measured using a commercial ELISA kit (CUSABIO, Wuhan, China; catalog no. CSB-E08490h) according to the manufacturer's protocol. Each sample was assayed in duplicate, and the intra-assay coefficients of variation were < 10%. Absorbance at 450 nm was measured using a BioTek Synergy H1 microplate reader (BioTek Instruments, Winooski, USA).

Statistical analysis

Continuous data are presented as mean ± SD for normally distributed data or median with interquartile range for non-normally distributed data. Between-group comparisons were performed using Student's t-test or Wilcoxon rank-sum test, as appropriate. Categorical variables are presented as counts and percentages, and are compared using the Pearson chi-square test, Yates' continuity corrected chi-square test, or Fisher's exact test, as appropriate. Normality was assessed using the Shapiro-Wilk test. Correlation analyses were performed using Pearson or Spearman rank correlation coefficients for normally or non-normally distributed data, respectively. Statistical analyses and data visualization were conducted using R software (version 4.3.2) with the *ggplot2*, *cowplot*, and *ComplexHeatmap* packages. All statistical tests were two-sided, with $P < 0.05$ considered statistically significant.

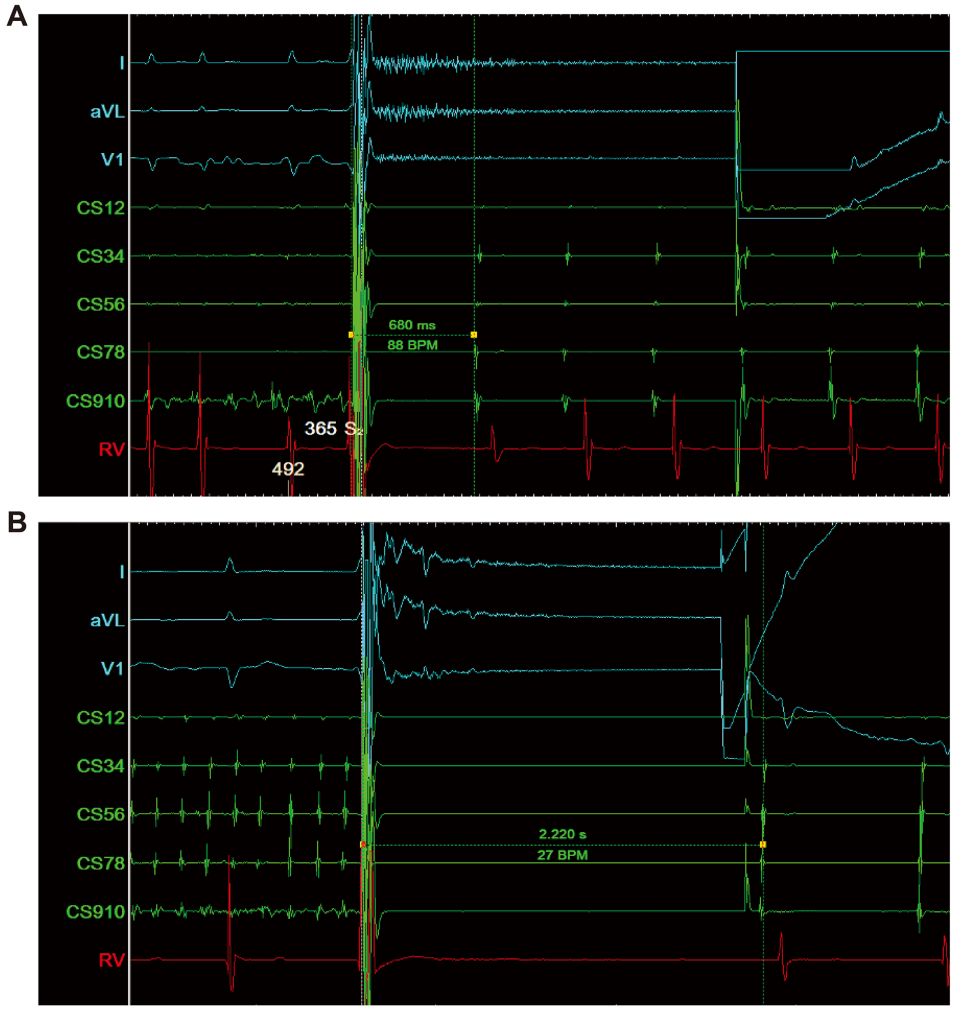

Figure 2. Intracardiac electrograms showing normal (A) and prolonged (B) sinus node recovery times (SNRT) after electrical cardioversion. (A) Example of normal sinus node recovery following direct current cardioversion. The first spontaneous sinus P wave appeared 680 ms after the cardioversion shock. (B) Example of delayed sinus node recovery after cardioversion. The first sinus P wave appeared 2.22 s after the shock. CS: coronary sinus electrograms recorded from proximal (CS12) to distal (CS910) poles; I: aVL, V1, surface ECG leads; RV: right ventricular channel.

RESULTS

Baseline characteristics

A total of 226 patients with PerAF were screened according to the predefined inclusion and exclusion criteria [Figure 1], of whom 177 met the eligibility criteria and were included in the study. Based on SNRT measured immediately after PVI and synchronized cardioversion, participants were stratified into the prolonged-SNRT group (SNRT ≥ 1,500 ms) and the normal-SNRT group (SNRT < 1,500 ms) [Figure 2]. Among the 177 eligible patients, 59 patients (33%) had prolonged SNRT, whereas the remaining 118 (67%) patients had normal SNRT.

Baseline demographic characteristics, comorbidities, echocardiographic parameters, and medication use are summarized in Table 1. The sinus rate after cardioversion was significantly lower in patients with prolonged SNRT, whereas all other baseline parameters were comparable between the two groups. To minimize potential confounding, PSM was performed, resulting in 56 matched pairs with excellent covariate balance [Table 2, Supplementary Figure 1A and B], thereby ensuring balanced baseline characteristics for subsequent analyses.

Table 1. Baseline clinical characteristics before matching on the propensity score

Variables	Total *n* = 177 (%)	SNRT ≥ 1,500 ms *n* = 59 (%)	SNRT < 1,500 ms *n* = 118 (%)	*P* value
Age, years	63.88 ± 9.56	63.71 ± 10.21	63.97 ± 9.26	0.988[a]
Male, n (%)	122 (68.9)	40 (67.8)	82 (69.5)	0.954[b]
BMI, kg/m^2	25.57 ± 3.57	25.35 ± 3.62	25.68 ± 3.55	0.561[c]
Smoke, n (%)	45 (25.4)	11 (18.6)	34 (28.8)	0.200[b]
Drink, n (%)	53 (29.9)	17 (28.8)	36 (30.5)	0.954[b]
Medical history, n (%)				
Hypertension	105 (59.3)	31 (52.5)	74 (62.7)	0.256[b]
DM	38 (21.5)	16 (27.1)	22 (18.6)	0.271[b]
CHD	54 (30.5)	16 (27.1)	38 (32.2)	0.604[b]
Stroke/TIA	20 (11.3)	5 (8.5)	15 (12.7)	0.557[b]
Medications, n (%)				
ACEI/ARB/ARNI	73 (41.2)	18 (30.5)	55 (46.6)	0.059[b]
β-Blocker	75 (42.4)	26 (44.1)	49 (41.5)	0.872[b]
DHP-CCB	61 (34.4)	19 (32.2)	42 (35.6)	0.780[b]
Diuretics	28 (15.8)	6 (10.2)	22 (18.6)	0.216[b]
Antiarrhythmics (Class I, III and IV)	12 (6.8)	5 (8.5)	7 (5.9)	0.751[d]
Cardiac glycosides	11 (6.2)	2 (3.4)	9 (7.6)	0.427[e]
eGFR (ml/min/1.73m^2)	76.51 ± 17.03	78.10 ± 17.71	75.73 ± 16.72	0.400[c]
ALT (IU/L)	23.62 ± 15.32	25.69 ± 18.03	22.60 ± 13.76	0.227[c]
AST (IU/L)	25.50 ± 11.06	25.61 ± 10.32	25.44 ± 11.45	0.925[c]
LAD, mm	45.19 ± 2.85	45.31 ± 3.01	45.13 ± 2.78	0.647[a]
LVEF, %	61.25 ± 7.42	61.36 ± 7.05	61.20 ± 7.62	0.914[a]
Heart rate, bpm	78.02 ± 15.07	74.46 ± 15.55	79.81 ± 14.57	0.028[a]

Data are presented as mean ± SD or a percentage. [a]Wilcoxon rank-sum test; [b]Pearson's $\chi 2$ test; [c]Student's t-test; [d]Yates' $\chi 2$ test; [e]Fisher's exact test. ACEI: angiotensin converting enzyme inhibitor; ARB: angiotensin receptor blocker; ARNI: angiotensin receptor neprilysin inhibitor; BMI: body mass index; CHD: coronary heart disease; DHP-CCB: dihydropyridine calcium channel blocker; DM: diabetes mellitus; LAD: left atrial diameter; LVEF: left ventricular ejection fraction; SNRT: sinus node recovery time; TIA: transient ischemic attack; eGFR: estimated glomerular filtration rate; ALT: alanine aminotransferase; AST: aspartate aminotransferase.

Relationship between SNRT and sinus rate

A statistically significant inverse association was observed between sinus rate after cardioversion and SNRT [Figure 3]. This finding demonstrated that slower intrinsic sinus rates are associated with longer recovery time and supported the value of prolonged SNRT as an indicator of SND.

Plasma proteomic profiling reveals an SND-associated molecular signature

To identify potential molecular biomarkers of SND, label-free plasma proteomic profiling was conducted in 10 discovery samples comprising five randomly selected patients from each group in the matched cohort. Quality-control analyses, including distributional assessment and missing-value filtering, revealed no apparent outliers or batch effects [Supplementary Figure 2A and B]. Principal component analysis (PCA) showed separation between the prolonged-SNRT and normal-SNRT samples along the main components [Figure 4A]. Using predefined thresholds, we identified 435 DEPs, including 138 upregulated and 297 downregulated proteins in the prolonged-SNRT group [Figure 4B]. Unsupervised clustering of these DEPs revealed clear group-coherent clusters [Figure 4C], supporting a biological divergence between the two groups. Functional enrichment analysis showed that upregulated proteins were mainly associated with

Table 2. Baseline clinical characteristics after matching on the propensity score

Variables	Total *n* = 112 (%)	SNRT ≥ 1,500 ms *n* = 56 (%)	SNRT < 1,500 ms *n* = 56 (%)	*P* value
Age, years	64.05 ± 9.82	63.46 ± 10.11	64.64 ± 9.58	0.588[a]
Male, n (%)	77 (68.8)	38 (67.8)	39 (69.6)	1[b]
BMI, kg/m^2	25.35 ± 3.28	25.56 ± 3.53	25.13 ± 3.03	0.490[c]
Smoke, n (%)	20 (17.8)	11 (19.6)	9 (16.1)	0.805[b]
Drink, n (%)	34 (30.4)	17 (30.4)	17 (30.4)	1[b]
Medical history, n (%)				
Hypertension	60 (53.6)	30 (53.6)	30 (53.6)	1[b]
DM	30 (26.8)	15 (26.8)	15 (26.8)	1[b]
CHD	31 (27.7)	15 (26.8)	16 (28.6)	1[b]
Stroke/TIA	12 (10.7)	5 (8.9)	7 (12.5)	0.760[b]
Medications, n (%)				
ACEI/ARB/ARNI	37 (33.0)	18 (32.1)	19 (33.9)	1[b]
β-Blocker	49 (43.8)	25 (44.6)	24 (42.8)	1[b]
DHP-CCB	35 (31.2)	19 (33.9)	16 (28.6)	0.684[b]
Diuretics	13 (11.6)	6 (10.7)	7 (12.5)	1[b]
Antiarrhythmics (Class I, III and IV)	10 (8.9)	4 (7.1)	6 (10.7)	0.740[d]
Cardiac glycosides	4 (3.6)	2 (3.6)	2 (3.6)	1[e]
eGFR (ml/min/1.73m^2)	76.92 ± 17.39	78.19 ± 17.90	75.70 ± 16.95	0.463[c]
ALT (IU/L)	24.57 ± 15.60	24.84 ± 16.93	24.30 ± 14.28	0.862[c]
AST (IU/L)	25.11 ± 9.67	25.19 ± 9.87	25.04 ± 9.56	0.936[c]
LAD, mm	45.23 ± 2.91	45.25 ± 3.07	45.21 ± 2.77	0.925[a]
LVEF, %	60.95 ± 7.46	61.07 ± 7.11	60.82 ± 7.85	0.919[a]
Heart rate, bpm	77.20 ± 14.58	74.79 ± 14.60	79.61 ± 14.30	0.080[c]

Data are presented as mean ± SD or a percentage. [a]Wilcoxon rank-sum test; [b]Pearson's χ^2 test; [c]Student's t-test; [d]Yates' χ^2 test; [e]Fisher's exact test. ACEI: Angiotensin converting enzyme inhibitor; ARB: angiotensin receptor blocker; ARNI: angiotensin receptor neprilysin inhibitor; BMI: body mass index; CHD: coronary heart disease; DHP-CCB: dihydropyridine calcium channel blocker; DM: diabetes mellitus; LAD: left atrial diameter; LVEF: left ventricular ejection fraction; SNRT: sinus node recovery time; TIA: transient ischemic attack; eGFR: estimated glomerular filtration rate; ALT: alanine aminotransferase; AST: aspartate aminotransferase.

extracellular matrix (ECM) organization and collagen assembly, whereas downregulated proteins were enriched in oxidative phosphorylation and mitochondrial metabolic pathways [Figure 4D and E]. A protein-protein interaction network constructed from the DEPs [Figure 4F] showed high-degree hubs in inflammation and matrix remodeling clusters, consistent with matrix remodeling observed in enrichment analyses.

Co-expression network analysis identifies SND-associated modules

To characterize the modular organization of the proteome, WGCNA was performed using all quantified proteins. Sample clustering identified no outliers [Figure 5A]. Using a soft-thresholding power of β = 5 based on the scale-free topology criterion [Supplementary Figure 3A], the network was partitioned into multiple color-coded modules of varying sizes [Figure 5B and C]. Module-trait correlation analysis identified two modules associated with the prolonged-SNRT phenotype [Figure 5D]. The brown module was positively correlated with prolonged SNRT (r = 0.64, *P* = 0.04), whereas the green module was negatively correlated with the prolonged-SNRT phenotype (r = -0.86, *P* = 0.001). Eigengene dendrogram and adjacency heatmap analysis further showed that these modules formed distinct eigengene clusters, supporting coordinated proteomic programs associated with the prolonged-SNRT phenotype [Figure 5E].

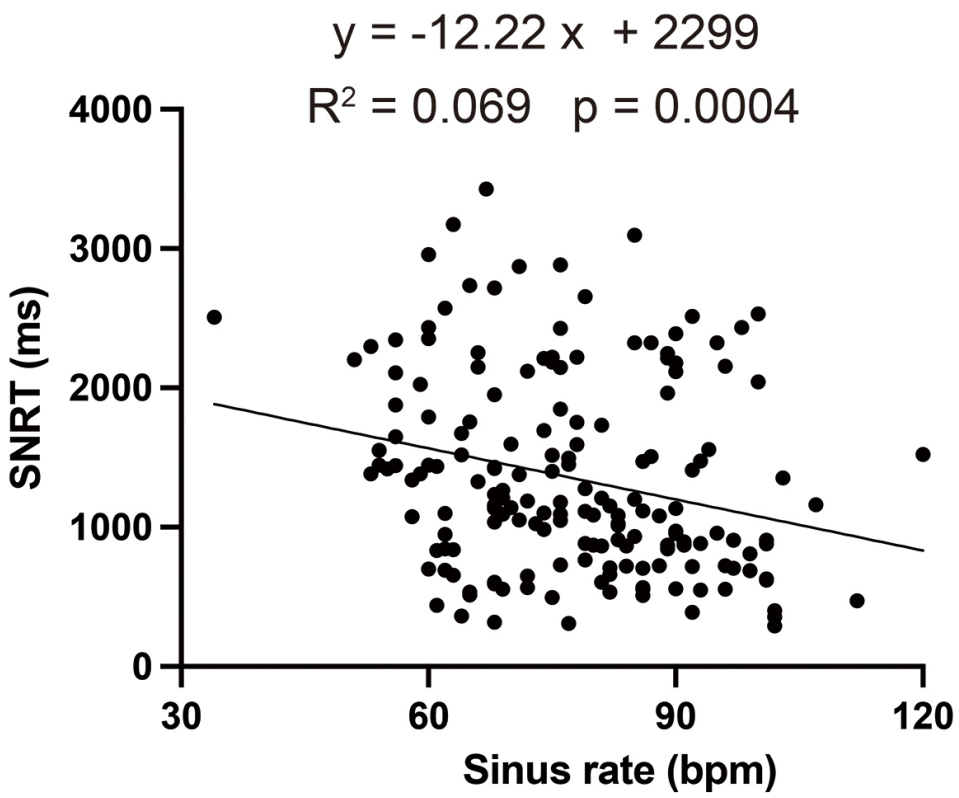

Figure 3. Relationship between SNRT and sinus rate after cardioversion. Pearson correlation analysis was performed, and the solid line represents the fitted linear regression line.

Within each SND-associated module, MM was strongly correlated with GS [Figure 5F], indicating that topologically central proteins tend to be the most trait-informative. Functional dot plots [Figure 5G] summarized the GO and KEGG themes for these modules, aligning closely with the DEP-level enrichment shown in Figure 4. To further visualize network interconnectivity, a TOM plot was constructed based on protein dissimilarity. In the resulting heatmap, lighter colors indicate stronger topological overlap and higher levels of co-expression among proteins within identified modules, whereas progressively darker red colors indicate weaker overlap [Supplementary Figure 3B]. Modules other than brown/green are shown in Supplementary Figure 3C and D to complete the network survey.

Elevated ACP5 was revealed as a candidate biomarker associated with prolonged SNRT

ECM and collagen-assembly features differed consistently between the two groups across both analytical approaches, suggesting that ECM remodeling may be one of the biological processes associated with prolonged SNRT in patients with PerAF. ACP5, a protein previously implicated in cardiac fibrosis, was identified as a consistently robust hub overlapping both DEP and WGCNA analysis [Figure 4B; Figure 5F]. ACP5 was therefore selected for orthogonal clinical validation.

ELISA was performed for ACP5 in the full matched cohort (56 matched pairs; $n = 112$). ACP5 levels were significantly elevated in patients with prolonged SNRT compared with those with normal SNRT [Figure 6A]. However, plasma ACP5 levels were not significantly correlated with SNRT duration when SNRT was analyzed as a continuous variable (Pearson r = 0.088, $R^2 = 0.008$, $P = 0.528$; Figure 6B).

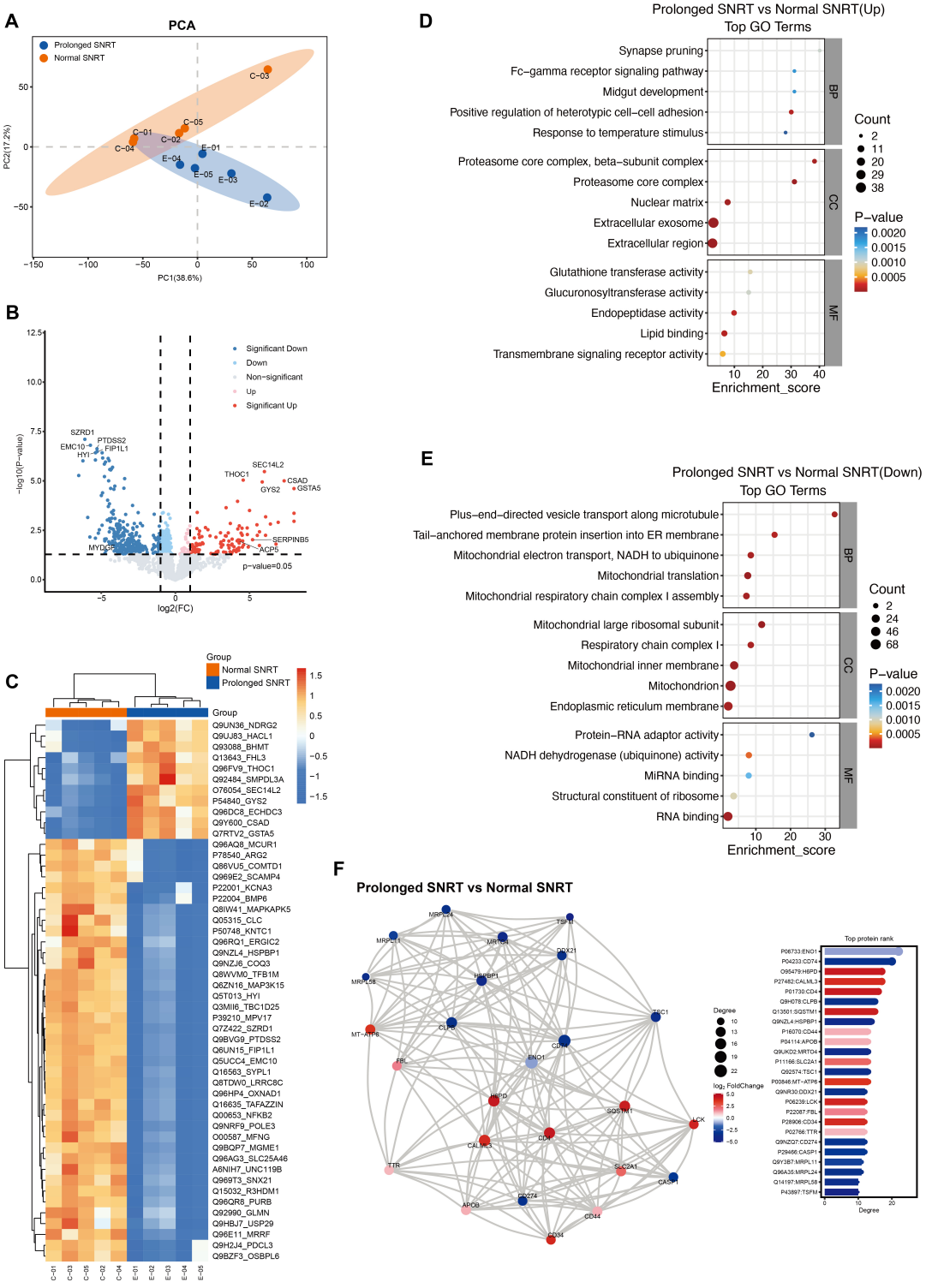

Figure 4. Proteomic profiling reveals distinct molecular signatures between the prolonged-SNRT and normal-SNRT groups. (A) Principal component analysis (PCA) showing clear separation between prolonged-SNRT and normal-SNRT samples. (B) Volcano plot showing significantly upregulated and downregulated proteins between the two groups. (C) Heatmap of the top 50 DEPs demonstrating distinct group-specific expression patterns. (D) Gene ontology (GO) enrichment analysis summarizing the main biological processes associated with upregulated DEPs. (E) GO enrichment analysis summarizing the main biological processes associated with downregulated DEPs. (F) Protein-protein interaction (PPI) network visualizing the interaction landscape among DEPs. DEPs were defined as those with |log2 fold change| > 1 and $P < 0.05$.

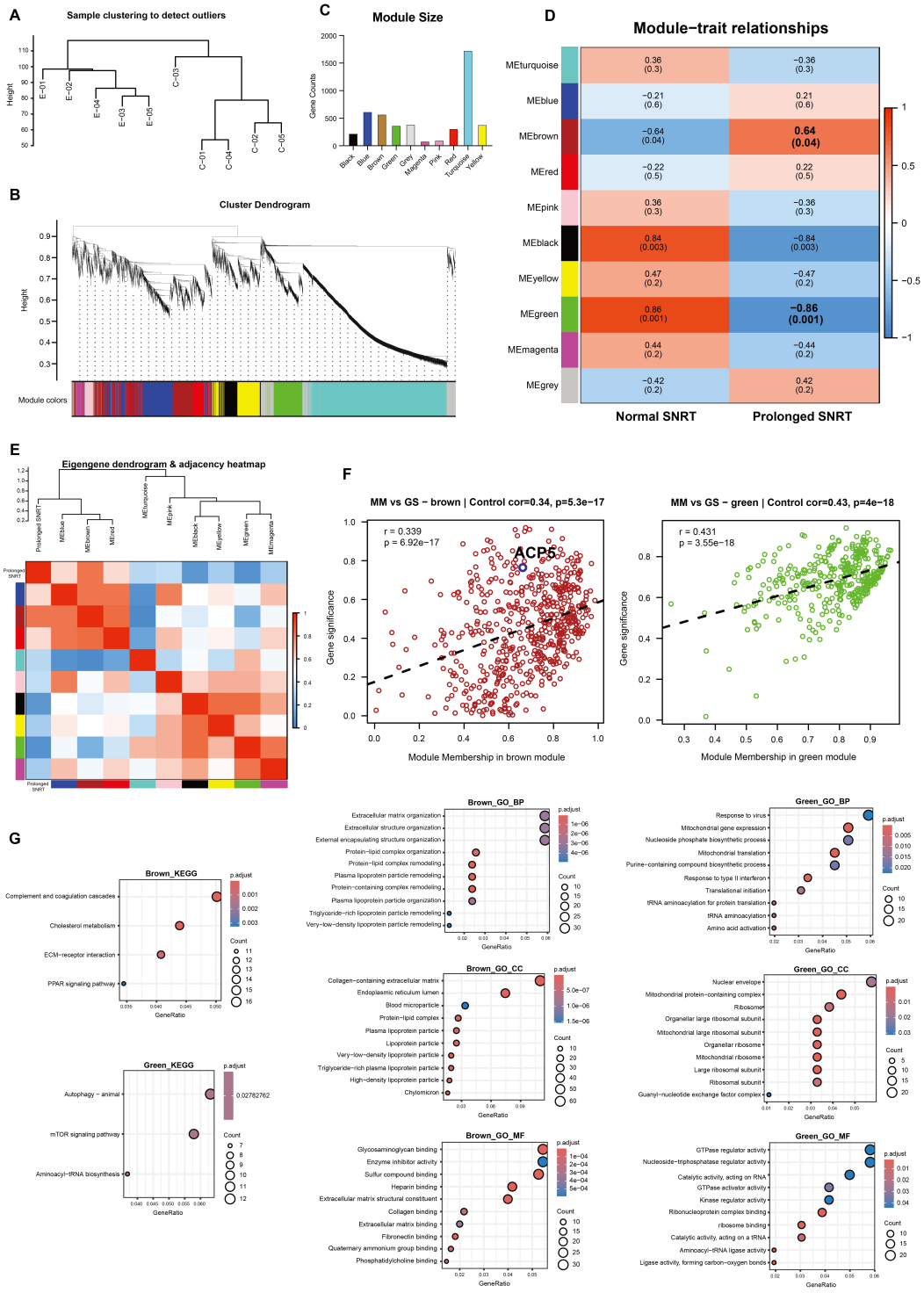

Figure 5. Weighted protein co-expression network analysis (WGCNA) and functional characterization of key modules. (A) Sample clustering dendrogram of all proteomic samples before network construction, showing no apparent outliers. (B) Cluster dendrogram of proteins with module color assignment. (C) Bar plot summarizing the number of proteins assigned to each co-expression module, with colors representing module identities. (D) Heatmap of module-trait correlations illustrating Pearson coefficients between module eigengenes and the prolonged-SNRT phenotype (prolonged vs. normal SNRT). (E) Eigengene dendrogram and adjacency heatmap showing relationships among module eigengenes. (F) Scatterplots illustrating the relationship between module membership (MM) and gene significance (GS) for the brown and green modules. Each dot represents a protein, and positive correlations indicate that highly connected proteins are closely associated with the phenotype. (G) GO and KEGG enrichment analyses of the brown and green modules, highlighting the top-enriched biological processes, cellular components, molecular functions, and pathways relevant to the prolonged-SNRT phenotype.

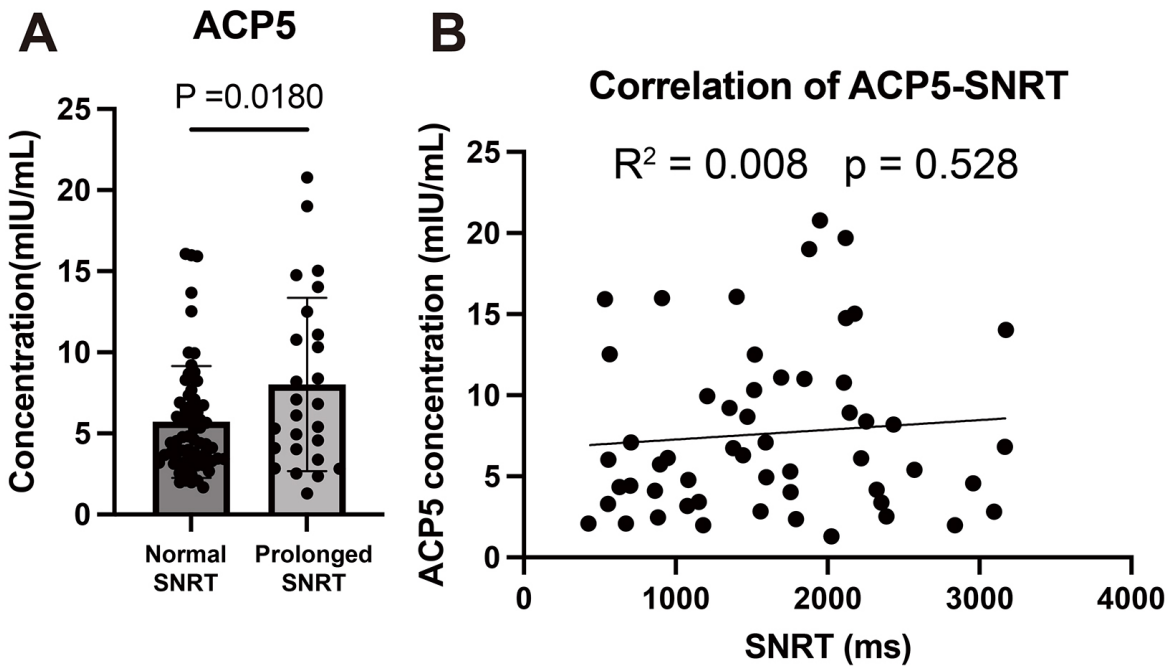

Figure 6. ELISA assessment of plasma ACP5 in the matched cohort. (A) Plasma levels of ACP5 were compared between the normal-SNRT and prolonged-SNRT groups. Data are presented as mean ± SD. Statistical significance was assessed using an unpaired two-tailed Student's t-test. (B) Correlation between plasma ACP5 concentration and SNRT duration in the matched cohort. The association was evaluated using Pearson correlation analysis. ACP5, acid phosphatase 5.

DISCUSSION

In this study, a combined clinical-proteomic framework was established to elucidate molecular signatures associated with prolonged SNRT among patients with PerAF. By integrating intra-procedural electrophysiological assessment, quantitative plasma proteomics, and network-level systems analysis, the present work provides a multidimensional characterization of the remodeling processes associated with impaired sinus node function.

The combined proteomic and WGCNA findings suggest that fibrotic remodeling may represent an important biological process underlying impaired sinus node function. Specifically, the upregulation of ECM components and matrix-remodeling proteins indicates a structural remodeling toward a profibrotic state. Such structural alterations are well-documented to disrupt cardiac pacemaker cell automaticity and electrical conduction[14]. In contrast, the downregulated mitochondrial and translational pathways in the green module may reflect energetic insufficiency and cellular stress adaptation[15,16].

From a mechanistic standpoint, the dual signature of ECM activation and mitochondrial downregulation indicates a potential model in which altered structural-metabolic coupling may be associated with prolonged SNRT. PerAF-associated oxidative stress and local inflammation may promote fibroblast proliferation within the atrium, including the sinoatrial node region, impairing impulse initiation. These insights align with previous evidence of sinus node fibrosis in the setting of AF and reinforce the notion that SND and AF mutually reinforce disease progression[5,15].

Our study suggests that plasma proteomic signatures may provide molecular insights into biological processes associated with prolonged SNRT in patients with PerAF. Among the candidate DEPs, ACP5 emerged as a prominent candidate biomarker within the brown co-expression module strongly associated with the prolonged-SNRT phenotype. ACP5 may serve as a circulating indicator of inflammatory and

matrix-remodeling activity related to impaired sinus node recovery. However, the absence of a significant linear correlation between ACP5 concentration and SNRT duration indicates that ACP5 should not be interpreted as a quantitative marker of the severity of sinus node recovery impairment. Instead, the present findings support its further evaluation as a candidate circulating biomarker associated with sinoatrial node function.

ACP5 encodes tartrate-resistant acid phosphatase 5, a lysosomal enzyme involved in bone resorption and immune-cell activation[17]. Increasing evidence supports its involvement in cardiac fibrosis and macrophage-mediated remodeling[18]. ACP5 has been proposed as a marker of systemic inflammatory burden across chronic disease states. Critically, its plasma concentration has been shown to exhibit a strong correlation with the degree of coronary atherosclerosis[19]. Its elevation in plasma may reflect myocardial matrix turnover and macrophage activation accompanying SND. If validated in larger independent cohorts, ACP5 may have potential value in the assessment of sinoatrial node function in patients with PerAF.

Several limitations of this study should be acknowledged. First, this study included a relatively small proteomic discovery cohort and a single-center validation cohort, without independent multicenter validation or detailed diagnostic performance assessment. In addition, differential protein screening was based on nominal *P* values without correction for multiple comparisons, which may have increased the risk of false-positive findings. Therefore, the identified proteins should be interpreted as exploratory candidates requiring validation in larger independent cohorts. Accordingly, plasma ACP5 should be regarded as a candidate molecular biomarker associated with prolonged SNRT and sinoatrial node function rather than a validated diagnostic or screening marker for SND. Second, plasma proteomic profiles may not directly reflect sinoatrial nodal tissue biology, and the cross-sectional nature of the study precludes causal inference. It remains unclear whether ACP5 contributes directly to impaired sinus node recovery or represents a secondary response to disease progression. Finally, despite the use of a low-abundance protein enrichment strategy, some biologically relevant proteins may have remained underrepresented. Future studies incorporating larger independent cohorts and mechanistic gain- and loss-of-function experiments are needed to clarify the role of ACP5 in sinus node remodeling and its relationship with impaired sinus node function in patients with PerAF.

Conclusion

In conclusion, this study identifies a distinct plasma proteomic signature associated with prolonged SNRT in patients with PerAF. Using DIA-based proteomics and WGCNA, ACP5 was identified as a candidate plasma biomarker associated with prolonged SNRT. Collectively, these findings provide exploratory evidence that plasma ACP5 may serve as a candidate biomarker for assessing sinoatrial node function in patients with PerAF before rhythm control therapy.

DECLARATIONS

Authors' contributions

Conceptualization: Xie Y, Wu L, Zhang N
Methodology: Lin T, Zhou T, Lan Y, Wei Y, Bao Y
Investigation: Lin T, Zhou T, Jin Q
Visualization: Lin T, Lan Y, Luo Q, Lin C
Funding acquisition: Xie Y, Wu L
Project administration: Xie Y, Bao Y, Jin Q
Supervision: Bao Y, Lin C, Jin Q, Zhang N
Writing - original draft: Lin T, Lan Y
Writing - review & editing: Zhou T, Xie Y

Availability of data and materials

The datasets used and analyzed during the current study are available from the corresponding author on

reasonable request.

AI and AI-assisted tools statement

During the preparation of this manuscript, the AI tool ChatGPT (GPT-5.1, OpenAI; released 2025-11-12) was used solely for creating the graphic abstract. The tool did not influence the study design, data collection, analysis, interpretation, or the scientific content of the work. All authors take full responsibility for the accuracy, integrity, and final content of the manuscript.

Financial support and sponsorship

This work was supported by the National Natural Science Foundation of China (grant number 82100329) and the foundation of Specialized Disease Diagnosis and Treatment Centers of Shanghai Jiao Tong University School of Medicine (YW0019).

Conflicts of interest

All authors declared that there are no conflicts of interest.

Ethical approval and consent to participate

The study protocol conformed to the Declaration of Helsinki and was approved by the Institutional Ethics Committee of Ruijin Hospital, Shanghai Jiao Tong University School of Medicine (Approval No. 2021-139). Written informed consent was obtained from all participants prior to enrollment.

Consent for publication

Not applicable.

Supplementary Materials

Supplementary Materials

REFERENCES

1. Kataoka S, Ejima K, Yazaki K, et al. Impact of atrial fibrillation ablation on long-term outcomes in patients with tachycardia-bradycardia syndrome. *J Arrhythm.* 2022;38:598-607. DOI PubMed PMC
2. Duan S, Du J. Sinus node dysfunction and atrial fibrillation—relationships, clinical phenotypes, new mechanisms, and treatment approaches. *Ageing Res Rev.* 2023;86:101890. DOI PubMed
3. Hwang TH, Yu HT, Kim T, et al. Permanent pacemaker implantations after catheter ablation in patients with atrial fibrillation associated with underlying sinus node dysfunction. *Korean Circ J.* 2020;50:346. DOI PubMed PMC
4. Lamas GA, Lee KL, Sweeney MO, et al. Ventricular pacing or dual-chamber pacing for sinus-node dysfunction. *N Engl J Med.* 2002;346:1854-62. DOI PubMed
5. John RM, Kumar S. Sinus node and atrial arrhythmias. *Circulation.* 2016;133:1892-900. DOI PubMed
6. Sairaku A, Nakano Y, Oda N, et al. Prediction of sinus node dysfunction in patients with long-standing persistent atrial fibrillation using the atrial fibrillatory cycle length. *J Electrocardiol.* 2012;45:141-7. DOI
7. Sunaga A, Masuda M, Kanda T, et al. A low fibrillatory wave amplitude predicts sinus node dysfunction after catheter ablation in patients with persistent atrial fibrillation. *J Interv Card Electrophysiol.* 2015;43:253-61. DOI
8. Motoda C, Nakano Y, Oda N, et al. Sleep-disordered breathing predicts sinus node dysfunction in persistent atrial fibrillation patients undergoing pulmonary vein isolation. *J Cardiol.* 2012;60:321-6. DOI
9. Bakhshi H, Michelhaugh SA, Bruce SA, et al. Association between proteomic biomarkers and myocardial fibrosis measured by MRI: the multi-ethnic study of atherosclerosis. *eBioMedicine.* 2023;90:104490. DOI PubMed PMC
10. Park H, Norby FL, Kim D, et al. Proteomic signatures for risk prediction of atrial fibrillation. *Circulation.* 2025;152:217-29. DOI PubMed PMC
11. Langfelder P, Horvath S. WGCNA: an R package for weighted correlation network analysis. *BMC Bioinformatics.* 2008;9:559. DOI PubMed PMC
12. Zhelyakov EG, Ardashev AV. Endocardial electrophysiological study in clinical practice in patients with bradysystole and conduction rhythm disorders: a review. *Cardiac Arrhythmias.* 2022;2:19-30. DOI

13. Pietrucha AZ, Wnuk M, WojewÓdka-Żak E, et al. Evaluation of sinus and atrioventricular nodes function in patients with vasovagal syncope. *Pacing Clin Electrophysiol.* 2009;32:S158-62. DOI
14. Mezzano V, Liang Y, Wright AT, et al. Desmosomal junctions are necessary for adult sinus node function. *Cardiovasc Res.* 2016;111:274-86. DOI PubMed PMC
15. Yaniv Y, Juhaszova M, Lyashkov AE, Spurgeon HA, Sollott SJ, Lakatta EG. Ca^{2+}-regulated-cAMP/PKA signaling in cardiac pacemaker cells links ATP supply to demand. *J Mol Cell Cardiol.* 2011;51:740-8. DOI
16. Ren L, Gopireddy RR, Perkins G, et al. Disruption of mitochondria-sarcoplasmic reticulum microdomain connectomics contributes to sinus node dysfunction in heart failure. *Proc Natl Acad Sci USA.* 2022;119:e2206708119. DOI PubMed PMC
17. Ren X, Shan W, Wei L, Gong C, Pei D. ACP5: its structure, distribution, regulation and novel functions. *Anti Cancer Agents Med Chem.* 2018;18:1082-90. DOI
18. Yang S, Pei L, Huang Z, et al. Inhibition of tartrate-resistant acid phosphatase 5 can prevent cardiac fibrosis after myocardial infarction. *Mol Med.* 2024;30:89. DOI PubMed PMC
19. Morisawa T, Nakagomi A, Kohashi K, Kusama Y, Shimizu W. Serum tartrate-resistant acid phosphatase-5b levels are associated with the severity and extent of coronary atherosclerosis in patients with coronary artery disease. *J Atheroscler Thromb.* 2017;24:1058-68. DOI PubMed PMC